Revista ALCONPAT
www.revistaalconpat.org
eISSN 2007-6835
Revista de la Asociación Latinoamericana de Control de Calidad, Patología y Recuperación de la Construcción

Development of lightweight ultra high performance concrete to architectural applications.

J. Xilotl-Dominguez[1]*, A. Duran-Herrera[1], L. López-Yépez[1], A. Muñoz-Espinoza[1]
*Contact author: jorge.a.x@hotmail.com
DOI: https://doi.org/10.21041/ra.v15i3.907

Received: 17/09/2024 | Received in revised form: 29/05/2025 | Accepted: 13/05/2025 | Published: 01/09/2025

ABSTRACT

This study aims to reduce the weight and enhance the thermal performance of Ultra-High-Performance Concrete (UHPC) for architectural applications while maintaining adequate mechanical strength. To achieve this, expanded polystyrene perlite (EPP) was used to replace limestone sand by mass (0, 30, 55, 80, and 100%) and synthetic Polyvinyl Alcohol (PVA) structural fiber was added. The mixes were evaluated for compressive and flexural strength, surface and bulk electrical resistivity, and thermal conductivity. Results showed that EPP significantly reduced density and thermal conductivity, while PVA improved strength. However, high EPP contents decreased mechanical performance. The combination of EPP and PVA in UHPC is innovative. It was concluded that optimized mixtures can balance thermal efficiency and structural integrity for architectural uses.

Keywords: lightweight UHPC; durability; thermal performance; electrical resistivity, PVA fibers.

Cite as: Xilotl-Domínguez, J., Durán-Herrera, A., López-Yépez, L., Muñoz-Espinoza, A. (2025), "*Development of lightweight ultra high performance concrete to architectural applications.*", Revista ALCONPAT, 15 (3), pp. 299 – 314, DOI: https://doi.org/10.21041/ra.v15i3.907

[1] Dpto de Tecnología del Concreto, Facultad de Ingeniería Civil, Universidad Autónoma de Nuevo León, Monterrey, México.

Contribution of each author
In this work, the author Xilotl-Dominguez contributed with the activity of the experimental development and the first sketch of the writing, the author Duran-Herrera (80%) and López-Yépez (20%) with the activity of the theoretical development of the experimental approach and guide of the article, as well as the original idea, writing of the work, discussion of results, among others. The author Muñoz-Espinoza collaborated by contributing materials in the experimental part and contributions about the methodologies to be followed.

Discussions and subsequent corrections to the publication
Any dispute, including the replies of the authors, will be published in the first issue of 2026 provided that the information is received before the closing of the third issue of 2025.

Desarrollo de concretos ligeros de ultra alto comportamiento para aplicaciones arquitectónicas.

RESUMEN

Este estudio busca reducir el peso y mejorar el rendimiento térmico del Concreto de Ultra Alto Comportamiento (UHPC) para aplicaciones arquitectónicas, manteniendo una resistencia mecánica adecuada. Para lograrlo, se utilizaron perlas de poliestireno expandido (EPP) para reemplazar la arena de piedra caliza (0, 30, 55, 80 y 100% en masa) y se añadieron fibras estructurales sintéticas de Alcohol Polivinílico (PVA). Las mezclas se evaluaron en resistencia a compresión y flexión, resistividad eléctrica superficial y volumétrica, y conductividad térmica. Los resultados mostraron que el EPP redujo significativamente la densidad y la conductividad térmica, mientras que el PVA mejoró la resistencia. Sin embargo, altos contenidos de EPP disminuyeron el desempeño mecánico. La combinación de EPP y PVA en UHPC es innovadora. Se concluyó que mezclas optimizadas pueden equilibrar eficiencia térmica e integridad estructural para usos arquitectónicos.

Palabras clave: concreto de ultra alto desempeño; durabilidad; resistividad eléctrica; Fibras PVA; propiedades térmicas.

Desenvolvimento de concreto leve de ultra alto desempenho para aplicações arquitetônicas.

RESUMO

Este estudo visa reduzir o peso e melhorar o desempenho térmico do Concreto de Ultra Alto Desempenho (UHPC) para aplicações arquitetônicas, mantendo resistência mecânica adequada. Para isso, perlita de poliestireno expandido (EPP) foi utilizada para substituir a areia de calcário em massa (0, 30, 55, 80 e 100%) e fibras estruturais sintéticas de Alcohol Polivinílico (PVA) foram adicionadas. As misturas foram avaliadas quanto à resistência à compressão e flexão, resistividade elétrica superficial e volumétrica, e condutividade térmica. Os resultados mostraram que o EPP reduziu significativamente a densidade e a condutividade térmica, enquanto o PVA aumentou a resistência. Contudo, altos teores de EPP diminuíram o desempenho mecânico. A combinação de EPP e PVA em UHPC é inovadora. Concluiu-se que misturas otimizadas podem equilibrar eficiência térmica e integridade estrutural para usos arquitetônicos.

Palavras-chave: UHPC leved; desempenho térmico; resistividade elétrica, fibras de PVA.

1. INTRODUCTION

In the construction industry, numerous materials and technologies have been proposed to improve construction processes and to optimize the use of the material. In this regard, Ultra-High-Performance Concretes (also known as UHPC) are those concretes with notable characteristics in terms of compressive strength, durability, and ductility. These concretes emerged in the 1980s as a solution to the search for high durability through the implementation of packing models, which allow reducing porosity by increasing the densification of the cement matrix, that make them highly durable against various external potential deterioration agents. Currently, among the applications in which these concretes are being widely used, architectural applications are becoming increasingly more prominent, due to their versatility in adopting shapes, textures, finishes, etc.

UHPC is a material that has attracted the interest of the research and construction industry because it can satisfy some issues such as slender elements, high durability and service life of more than 100 years (Azmee and Shafiq, 2018; Badogiannis, et al. 2021), as well as ductility due to the incorporation of steel fibers (Alkadhim, et al. 2022).

UHPCs are a cementitious composite material that has improved compressive strength, ductility and durability properties if compared with HPC. UHPCs can contain fibers for post-cracking ductility (Andrade and D'Andrea, 2011). UHPCs are those concretes that have at least a compressive strength ≥ 120 MPa cured under normal conditions and ≥ 150 MPa when steam cured, and a tensile strength ≥ 5 MPa (Badogiannis, et al. 2021).

Similarly, they have low water/binder ratios (0.15-0.25), high matrix packing (0.825-0.855), high steel fiber volumes (≥ 2%), and for their production it is mandatory the use of a high range water reducing admixture or superplasticizer to provide high flowability to the mixture (≥ 160 mm in the mini-cone) (Badogiannis, et al. 2021).

Lightweight concrete (LC) exhibits distinct properties compared to conventional concrete and UHPC, including lower density (typically 1,200–1,800 kg/m³) and enhanced thermal/acoustic insulation. Primary structural applications include slabs, wall fillings, and cladding panels, where its reduced weight lowers dead loads while improving fire resistance (Thienel, et al. 2020).

However, lightweight concrete is characterized by its low compressive strength and sometimes lower durability, due to the use of lightweight aggregates, foaming admixtures or air inclusions. Therefore, by substituting the typical cementitious matrix with a UHPC matrix it could be an attractive idea to exploit the strengths of both technologies.

Lightweight Ultra-High-Performance Concrete (also known as L-UHPC) is the combination of a conventional UHPC and the incorporation of lightweight aggregates, resulting in improved properties, so it must maintain properties and characteristics such as high matrix packing and low water/cement ratio (≤0.25), which allows maintaining durability properties even with a reduction in strength. Similarly, comparable density ranges for a L-UHPC could range between 1500 and 2000 kg/m^3 (Badogiannis, et al. 2021: Li, et al. 2022).

L-UHPCs retain the main matrix of an UHPC with the substitution of lightweight aggregate by normal weight aggregate. The main aggregates used in their manufacture are expanded clay, expanded glass beads, fly ash microspheres and expanded polystyrene perlite (EPP) (Shi, et al. 2018). Likewise, there are different fibers used in conventional UHPCs, the most common ones are usually steel, due to its tensile strength properties, that have high ductility (Shi, et al. 2018; Yang, et al. 2022). However, other fibers such as Polyvinyl Alcohol (PVA), Glass (G), Polyethylene (PE) and Polypropylene (PP) are also used (Shi, et al. 2018; Yang, et al. 2022; Abu, et al. 2022; Le and Fehling, 2017; Gong, et al. 2022).

As an effort to reduce maintenance costs, as well as to provide greater durability, long service life of the structure and to streamline constructability, projects around the world have sought to incorporate durability criteria's in the construction of infrastructure. Therefore, for projects that

require a durable, strong and ductile material, UHPCs could be the alternative of choice (Yang, et al. 2022; Habil and Fehling, 2005).

The main applications of UHPCs range from structural components, bridges, architectural elements, repair and rehabilitation, to vertical components for wind towers. However, the uses and applications are not limited and can include structural strengthening, retrofitting, prefabricated elements and other unique applications (Akeed, et al. 2022).

Also, the superior mechanical properties of UHPC enable the design and manufacture of slender, lightweight and aesthetically pleasing building components. For example, the Museum of European and Mediterranean Civilizations, the first building to make extensive use of UHPC, was built in 2013 in Marseille, France (Du, et al. 2021). Alternatively, the Jean Bouin stadium in Paris, which has 11,000 m^2 of Ultra-High Performance Fiber Reinforced Concrete (UHPFRC) panels on the sides and 10,000 m^2 on the roof (Mazzacane, et al. 2013).

Some authors have developed L-UHPC with different purposes, the main ones are due to the use of aggregates from local regions to reduce the cost of the final product (Wang, et al. 2021), and to improve the coefficient of thermal conductivity (Dixit, et al. 2019).

This work develops EPP-incorporated UHPC for architectural facades requiring <120 MPa strength but enhanced durability and ductility. The PVA fiber-reinforced system resists wind loads and environmental degradation while avoiding steel fiber corrosion (Kishore, et al. 2015).

In this work, five series of concretes were evaluated with substitutions of limestone sand by different percentages of EPP by volume (0, 30, 55, 80 and 100%) and the incorporation of a PVA. To evaluate the synergistic effect of EPP and PVA in a UHPC cementitious matrix the following properties were examined: compressive strength, flexural strength, surface electrical resistivity, bulk electrical resistivity and thermal conductivity.

2. MATERIALS AND METHODS

2.1 Materials

For the concrete production in this study, we utilized: white blended Portland cement (CPC 30R B, compliant with NMX-C-414); metakaolin (GCC-METAFORCE); calcite sand (maximum particle size 4.76 mm, #4 sieve); calcite filler (average particle size 5.91 µm, sourced from northeastern Mexico); expanded polystyrene perlite (EPP, maximum particle size 1 mm); and structural synthetic PVA fibers (KURALON K-II) specifically designed for UHPC applications. The PVA fibers, with average filament dimensions of 12 mm length and 200 µm diameter, were incorporated at 1.0%, 1.5%, and 2.0% by volume to determine the optimal dosage through beam bending tests.

To obtain a high flowability, an ether polycarboxylate based high-range water reducing or superplasticizer admixture (SP, FLOWCON P01) was used, and to improve the particle packing density a stabilizer was used to decrease the loss of consistency (STA, EUCON WORKONTROL), as well as an air excluder (EX, HDS ISODENSE 250) admixtures. Other physical properties of the materials are reported in Table 1.

Table 1. Complementary physical properties of the materials.

ID	Material	Density, g/cm^3	Absorption, %	d_{50}, µm	Length, mm	Diameter, mm	Solids content, %
CPC	Portland Cement	3.02	-----	18.16	-----	-----	-----
MK	Metakaolin	2.58	-----	16.66	-----	-----	-----
FA	Fine Aggregate	2.65	0.80	416.50	-----	-----	-----
F	Filler	2.67	-----	5.91	-----	-----	-----
EPP	Micro Expanded Polystyrene Perlite	5.5 x 10^{-2}	0.00	-----	-----	< 1.0	-----
PVA	Polyvinyl Alcohol Fiber	1.30	-----	-----	12.0	0.2	-----
SP	HRWRA/SP admix.	1.11	-----	-----	-----	-----	50.12
STA	Stabilizer admix.	1.10	-----	-----	-----	-----	40.00
EX	Air excluder admix.	0.98	-----	-----	-----	-----	35.00

2.2 Methodology

For a fixed water/cementitious (*w/cm*) ratio of 0.22, the optimization process to establish the reference mixture proportions, for a minimum compressive strength of 120 MPa and a target slump flow of 80 ± 2.5 cm, was determined according to the standard procedure. As described in ASTM C1611-21, the following dosages for CPC, MK, SP, STA and EX of 807.5 kg/m^3, 142.5 kg/m^3, 5.5 – 10.5 ml/kg of *cm*, 4.0 ml/kg of *cm* and 1.0 ml/kg of *cm* respectively, were prepared. The first methodology step in this work, was to obtain the mix design concrete, the properties in fresh and hardened concrete that were designed to obtain a minimum compressive strength of 120 MPa at 28 days in reference mix. Starting from the proportions of the reference mixture, four other mixtures were produced to evaluate the effect of EPP dosed in substitution of the limestone sand in the following percentages by volume: 30, 55, 80 and 100%. In this work, for the evaluation of these five mixtures they were labeled as R, MF3, MF5, MF8 and MF10, respectively.

To achieve the target slump flow of 80 ± 2.5 cm for the reference mixture, the superplasticizer (SP) dosage was 9.0 mL/kg of cementitious material (cm). This dosage decreased progressively with increasing EPP substitution: 8.3 mL/kg cm (30% EPP); 7.3 mL/kg cm (55% EPP); 6.8 mL/kg cm (80% EPP); and 5.2 mL/kg cm (100% EPP). These reductions also conduced to reductions in the slump flow within the range of 70 ± 5.0 cm. In comparison to the reference mixture, the incorporation of PVA fibers increases by 0.5 ml/0.5 % of PVA fiber the dosage of SP to maintain the slump flow.

For the determination of compressive strength, static modulus, surface and bulk electrical resistivity, and thermal conductivity, cylinders of 10 cm in diameter and 20 cm in height were prepared, according to the procedure described in ASTM C192-14 and, after preparation, kept in lime-saturated water under standard curing conditions (T = 23.0 ± 2.0°C, RH = ≥ 95%). For the determination of the compressive strength, the cylinders were tested by triplicate in an universal machine with a capacity of 200 tons, at the ages of 3, 7, 28 and 56 days, according to the standard procedure described in ASTM C39-21, and the averages of the results were used to construct the graphs shown in Figures 1 and 2. Compressive strength was determined by triplicate.

For the determination of the static modulus of elasticity, specimens were tested by triplicate according to the standard procedure described in ASTM C469-14, and the averages of the results

were used to construct the graph that appears in Figure 2.
For the determination of the flexural strength, prismatic specimens of 7.5 x 7.5 x 30.0 cm were cast, which were filled in a single layer and compacted by means of a vibrating table, with the minimum vibration intensity and for a period of 10 seconds. At an age between 24 and 30 hours, the specimens were demolded and immersed in lime-saturated water, under standard curing conditions (T = 23.0 ± 2.0°C, RH = ≥ 95%), until their flexural test age at 56 days, following the procedure described in UNE-EN 14651-2007. For this test, five specimens were cast for each of the concrete mixtures, and the average curves are shown in Figure 3.
Surface resistivity and bulk electrical resistivity were determined at 7, 28, and 56 days following the procedures described in AASTHO TP 95-14 and ASTM C1876-19, and the averages of the results were used to construct the graphs shown in Figure 4. Thermal conductivity was determined by the transient heat method on air-dry specimens at the age of 7 days, according to the standard procedure described in ASTM D5334-2, and the averages of the results were used to construct the graphs shown in Figure 5. Three specimens were cast to determine the thermal conductivity and the electrical resistivity.
The residual post-cracking strengths were determined by means of the bending test of the fiber-reinforced beams, which during their preparation were grooved with a diamond saw at the center of the span, according to the procedure described in UNE-EN 14651-2007, by means of which the load values and the corresponding progressive crack mouth openings (CMOD) were measured. The progressive widening of the crack mouth openings (CMOD) were acquired using an Epsilon brand clip strain gauge, model 3541, and a National Instruments brand data acquisition unit (DAQ), which was linked to a computer during the test using LabVIEW software.

3. RESULTS AND DISCUSSION

3.1 Compressive Strength

The main property that defines whether a concrete can be classified as a UHPC is the compressive strength, in this sense, in its report FHWA-HRt-13-060, the Federal Highway Administration of the United States of North America establishes that an UHPC should have a minimum strength of 120 MPa. For this work, the mixtures evaluated were manufactured from the proportions established for a UHPC in which white cement and limestone sand and powder from the metropolitan area of Monterrey, Mexico were used, with which compressive strengths of 105 and 140 MPa were obtained at ages of 28 and 56 days. However, to meet aesthetic objectives and trying to obtain a concrete whose color was as white as possible, for the five concretes evaluated in this study, the limestone sand and limestone powder were replaced by a white calcite, which was dosed in two fractions with the same particle sizes as the limestone powder and sand.

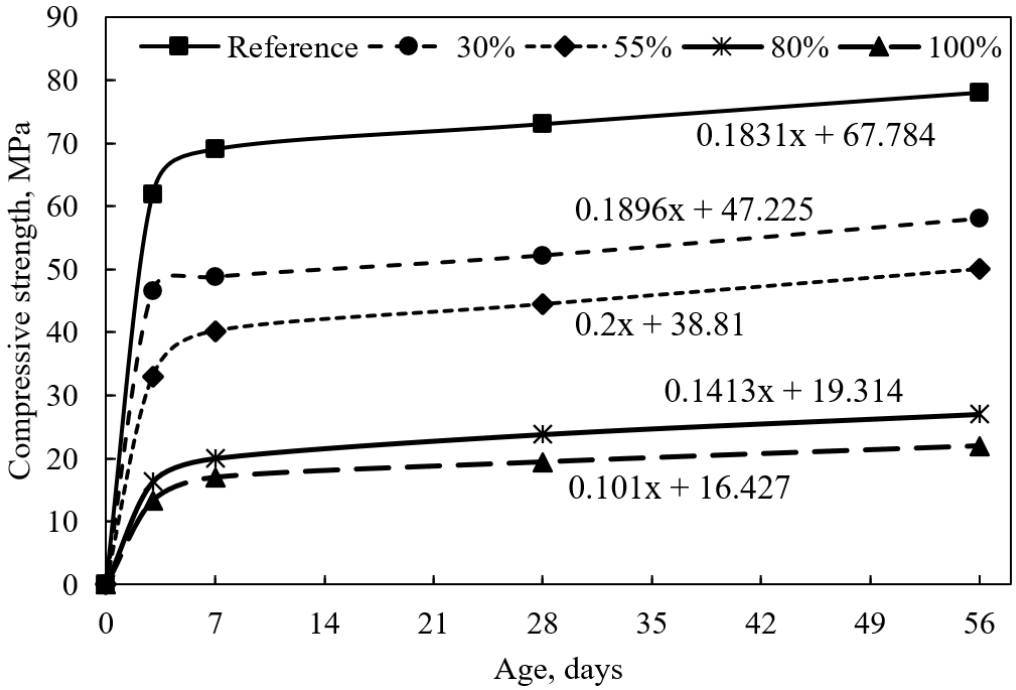

Figure 1. Compressive strength development for mixtures with EPP contents of 0, 30, 55, 80 and 100 %, by volume in substitution of the calcite sand and powder.

For the five mixtures evaluated in this study, figure 1 shows the compressive strength developments up to the age of 56 days. All mixtures exhibited significant early-age strength development, achieving 68.5-89.1% of their 28-day compressive strength within just three days. This rapid strength gain is attributed to the cement's high initial reactivity combined with the low water-cement ratio (w/c = 0.22). The three-day strength percentages relative to 28-day strength were: 84.4% (0% EPP), 89.1% (30% EPP), 74.3% (55% EPP), 68.5% (80% EPP), and 68.7% (100% EPP). In relation to the strengths corresponding to the age of 56 days, these gains were 79.4, 80.2, 66.0, 60.4 and 60.9 % respectively. Between the ages of 7 and 56 days, Figure 1 also clearly exhibits the pozzolanic effect of MK, by presenting increases in the development of compressive strength between this age range of 0.18, 0.19, 0.20, 0.14 and 0.10 MPa/day.

The substitution of calcite powder and calcite sand by different percentages of EPP, caused significant reductions in compressive strength, which increased as the percentage of EPP increased. In this sense, figure 2 indicates that each 1% increase in EPP substitution reduced compressive strength by 0.574 MPa. The most significant reduction occurred in the 100% EPP mixture, which achieved 22 MPa at 56 days. Notably, this mixture met the ACI 318-19 minimum structural requirement of 17 MPa by 7 days, demonstrating its suitability for structural applications despite the strength reduction.

3.2 Modulus of elasticity

In relation to the results obtained for the static modulus of elasticity at age 56 days (72.3 GPa), the results obtained for the substitutions of calcite by EPP presented significant reductions with average values of 50.1, 29.9, 23.6 and 15.1, for the mixtures with 0, 30, 55, 80 and 100 % of EPP, respectively. In this sense, figure 2 indicates that for each 1% substitution of calcite by EPP, the static modulus of elasticity will be reduced by 0.57 GPa.

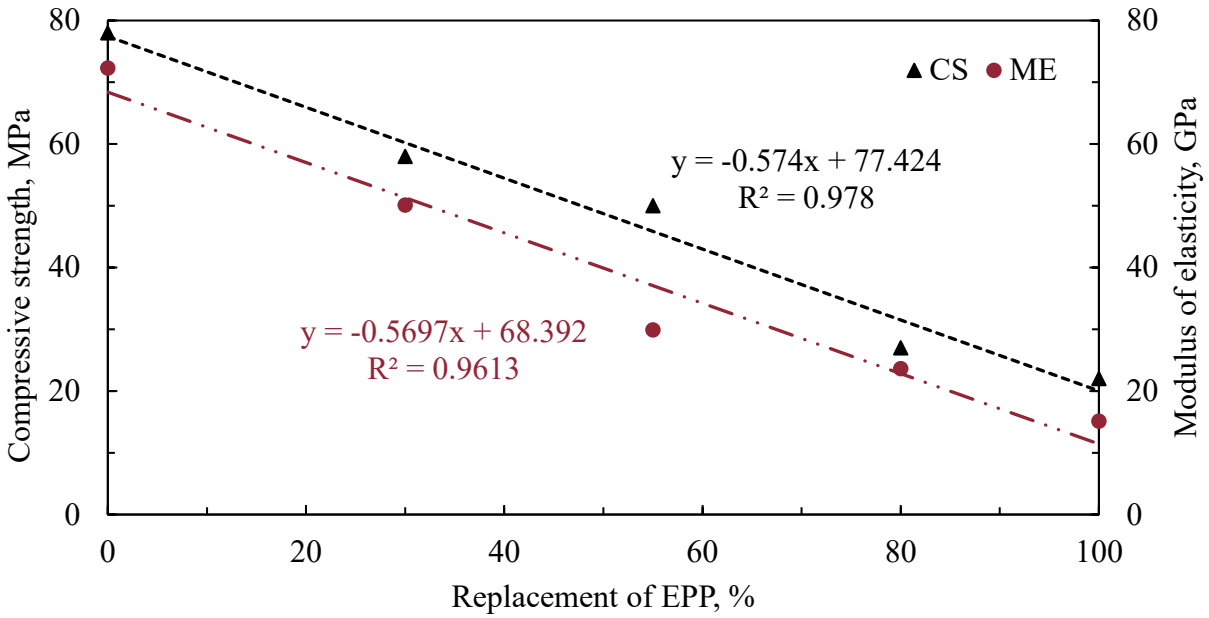

Figure 2. Effect of EPP additions on compressive strength (CS) and static modulus of elasticity (ME).

3.3 Flexural strength

In the construction industry, hydraulic concrete is a material that can currently be designed for compressive strengths between 20 and 200 MPa. This particular property is one of the positive qualities of the material, for the very diverse applications in which it is used, however, one of its great weaknesses is its tensile strength, which is usually counteracted by using steel rods, FRP rods, and metallic or synthetic fibers. Due to the ultra-high strength of UHPC, its cementitious matrix offers much better bonding capabilities with all these reinforcements, so the performance of the reinforcement is optimized, as is the case of the fibers in UHPC, a benefit that we can clearly observe in figure 3.

In the residual stress stage that occurs after the concrete presents the first crack, two types of behavior can be observed, the one known as strain softening, which is typical in conventional fiber-reinforced concretes and the one known as strain hardening, which is typical in high-strength concretes. The fracture mechanics involved in these behaviors depend on various factors of the fiber, such as the type of fiber, the dosed volume, the aspect ratio and the adhesion of the fiber with the cementitious matrix. In this sense, because the concretes studied in this research work are ultra-high-strength concretes, in the load-strain performances that are presented graphically in figure 3, three important stages are clearly distinguished during the development of the flexural test: a first phase that shows the maximum load when the first crack appears; a second phase that begins after the first phase ends and that shows a strain hardening attributable to the synergistic work of the fibers and the cementing matrix, right in the plane where the crack was induced; and a third phase that begins when the second phase ends and in which the strength is mainly driven by the strength of the fiber filaments that bridge the crack, and by the elasticity modulus of the material of which the fiber is composed.

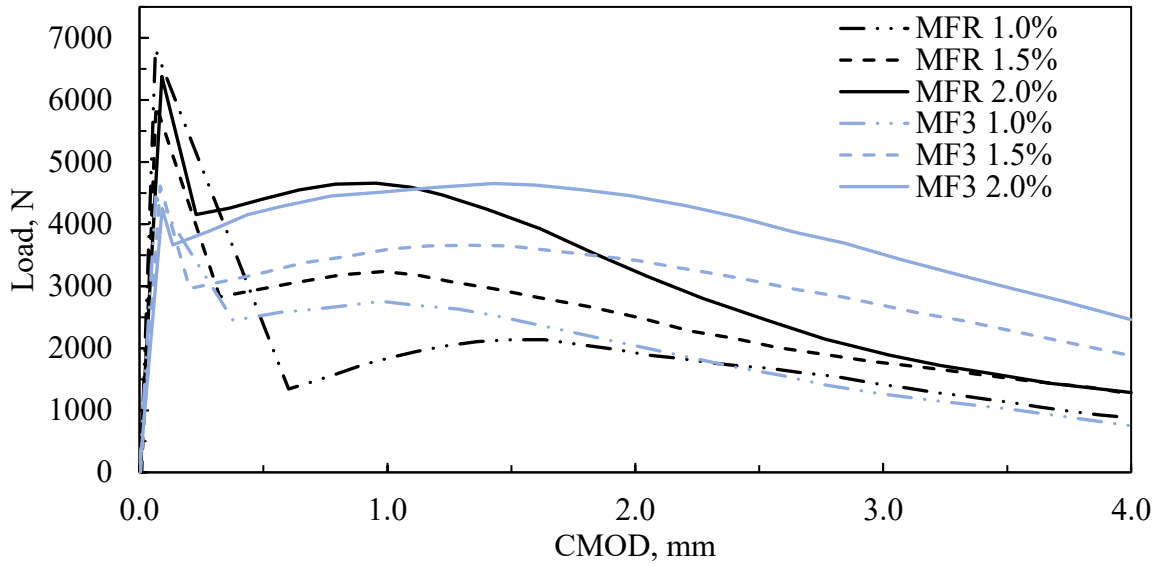
MFR 1.0%
MFR 1.5%
MFR 2.0%
MF3 1.0%
MF3 1.5%
MF3 2.0%
Load, N
CMOD, mm
0
1000
2000
3000
4000
5000
6000
7000
0.0
1.0
2.0
3.0
4.0

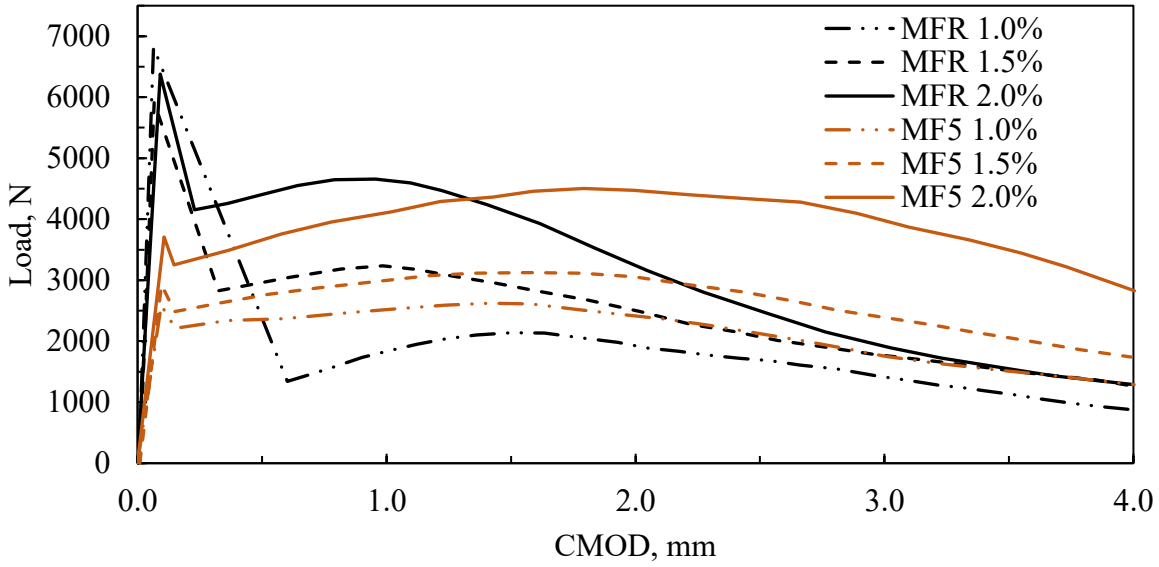
MFR 1.0%
MFR 1.5%
MFR 2.0%
MF5 1.0%
MF5 1.5%
MF5 2.0%
Load, N
CMOD, mm
0
1000
2000
3000
4000
5000
6000
7000
0.0
1.0
2.0
3.0
4.0

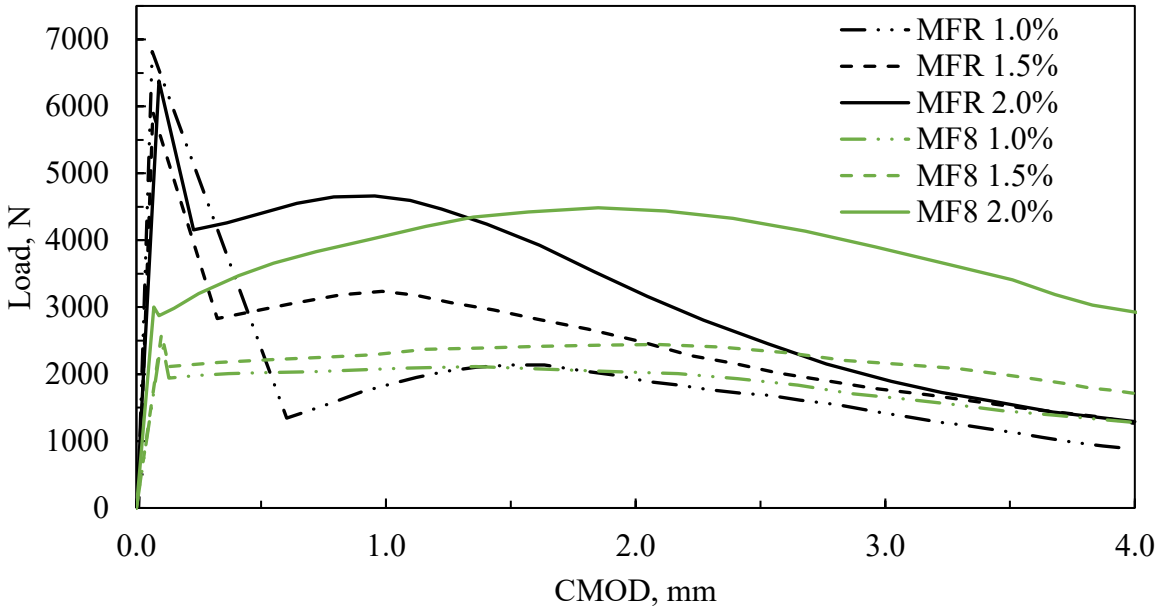
MFR 1.0%
MFR 1.5%
MFR 2.0%
MF8 1.0%
MF8 1.5%
MF8 2.0%
Load, N
CMOD, mm
0
1000
2000
3000
4000
5000
6000
7000
0.0
1.0
2.0
3.0
4.0

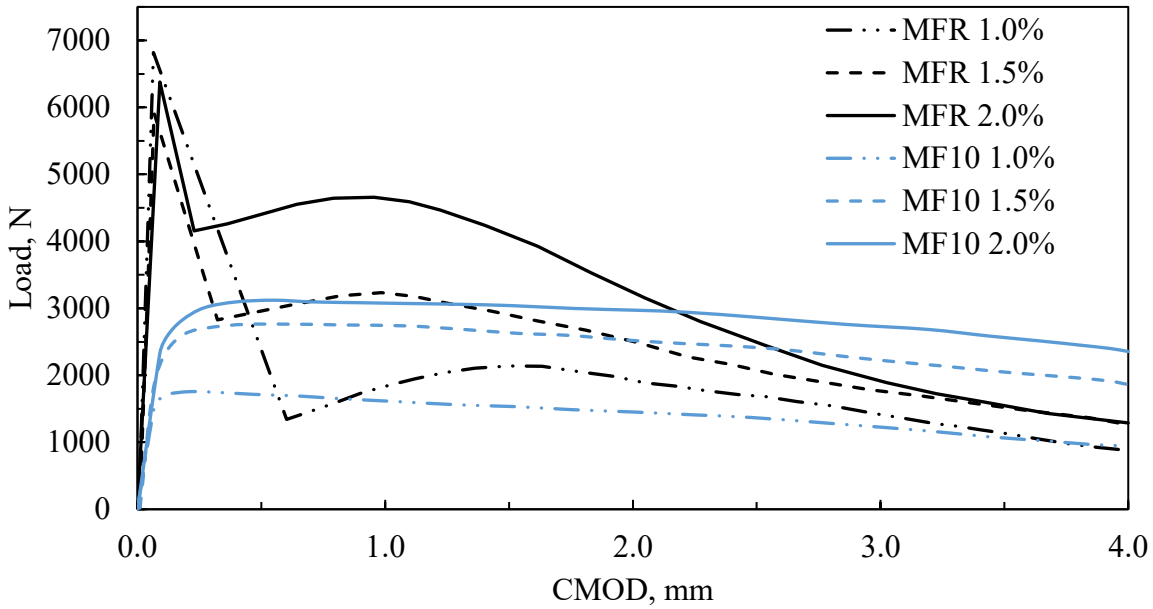

Figure 3. Load-CMOD curves of L-UHPC with: a) 30%, b) 55%, c) 80% and d) 100% of EPP replacement.

Figure 3 and table 3 present four comparisons between the average curves obtained through the flexural tests for mixture R and for each of the four mixtures with calcite substitutions for EPP, which are labeled as MF3, MF5, MF8 and MF10. For the three fiber dosages evaluated in this study (1.0, 1.5, and 2.0%), the graphs indicate that the maximum load at first crack occurred at CMOD values between 0.06 and 0.11 mm. The average first-crack loads were 6,371 N (R, 0% EPP), 4,434 N (MF3, 30% EPP), 3,074 N (MF5, 55% EPP), 2,232 N (MF8, 80% EPP), and 1,858 N (MF10, 100% EPP), with variations of ±450 N, ±180 N, ±500 N, ±155 N, and ±165 N, respectively. These results demonstrate progressive load reductions of 30%, 52%, 64%, and 71% for MF3, MF5, MF8, and MF10 compared to the reference mixture (R), directly attributable to EPP's near-zero compressive strength contribution.

For the 1.0% fiber dosage, the loads corresponding to the end of the strain hardening stage show a superior performance for the MF3, MF5 and MF8 mixtures, which presented results superior to those presented by the reference mixture, with increments of 29.0, 23.0 and 1.7%, respectively. On the other hand, mixture M10 presented a decrease of 17.8%. At this stage of the test and for this fiber dosage, it can be observed in these graphs that the deformations present CMOD values that are located between 0.21 and 1.72 mm.

For the 1.5% fiber dosage and in relation to the reference mixture, the loads corresponding to the end of the strain hardening stage show a superior performance of 13.14% only for mixture MF3, since mixtures MF5, MF8 and MF10 presented reductions of 3.4, 34.9 and 14.6%, respectively. At this stage of the test and for this fiber dosage, these graphs show that the deformations present CMOD values are between 0.62 and 1.58 mm.

Table 2. Comparative of different graphic points in different replacement of EPP.

% EPP	Mixture ID	A		B		C	
		P, N	CMOD, mm	P, N	CMOD, mm	P, N	CMOD, mm
0 (Reference)	MFR 1.0%	6818	0.06	2135	1.50	882	4.00
	MFR 1.5%	5915	0.07	3235	0.98	1262	
	MFR 2.0%	6379	0.09	4660	0.95	1288	
30 %	MF3 1.0%	4439	0.07	2754	0.97	749	4.00
	MF3 1.5%	4613	0.08	3660	1.32	1881	
	MF3 2.0%	4250	0.09	4654	1.43	2462	
55 %	MF5 1.0%	2589	0.09	2623	1.41	1289	4.00
	MF5 1.5%	2925	0.10	3124	1.58	1741	
	MF5 2.0%	3707	0.11	4503	1.79	2825	
80 %	MF8 1.0%	2486	0.10	2172	1.72	1255	4.00
	MF8 1.5%	2177	0.11	2106	1.53	1487	
	MF8 2.0%	2300	0.07	4485	1.85	2921	
100 %	MF1 1.0%	1667	0.07	1756	0.21	947	4.00
	MF1 1.5%	1904	0.07	2763	0.62	1855	
	MF1 2.0%	2003	0.09	3122	0.55	2355	

For the 2.0% fiber dosage and in relation to the reference mixture, the loads corresponding to the end of the strain hardening stage show an inferior performance for mixtures MF3, MF5, MF8 and M10, since they presented reductions of 0.13, 3.40, 3.76 and 33.00%. At this stage of the test and for this fiber dosage, these graphs show that the deformations present CMOD values that are between 0.55 and 1.85 mm.

For the fiber dosage of 1.0% and for a CMOD of 4 mm, the loads corresponding to the end of the strain softening stage were 15.08% lower for mixture MF3, and 46.15, 42.49 and 7.37% higher for mixtures MF5, MF8 and MF10, respectively.

For the 1.5 % fiber dosage and for a CMOD of 4 mm, in all cases the loads corresponding to the end of the strain softening stage were higher by 49.05, 37.96, 17.83 and 46.99 %, for mixtures MF3, MF5, MF8 and MF10, respectively. As for the 2.0 % fiber dosage and for a CMOD of 4 mm, at the end of this stage, in relation to the corresponding reference mixture, the increments were 91.15, 119.33, 126.79 and 82.84 %, for mixtures MF3, MF5, MF8 and MF10, respectively. These increments represent a significant increase in the energy absorption capacity to absorb energy when the material is under bending stresses, a benefit mainly attributed to the fibers.

3.4 Surface and bulk electrical resistivity (SER y BER)

The electrical resistivity of concrete is a parameter that reflects the densification level of the cementitious matrix in the concrete, because the denser the matrix, the greater the electrical resistivity of the material, and consequently the greater the material will be resistant to the entry of deleterious agents such as chlorides, sulfates, CO_2, humidity and others.

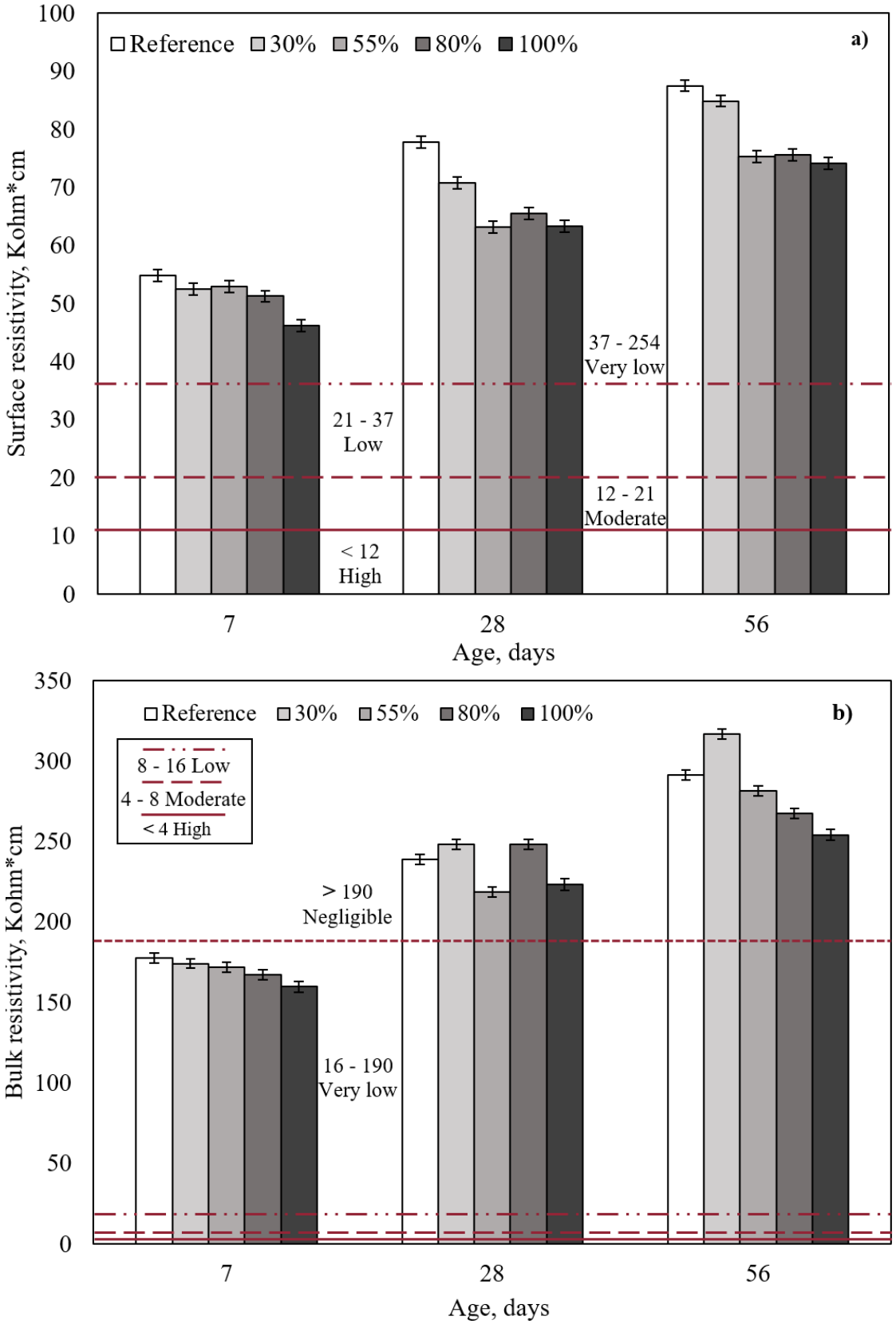

Figure 4. Surface (a) and bulk (b) electrical resistivities for the five concretes without fibers evaluated in this work.

Figure 4 presents the surface (SER) and bulk (BER) electrical resistivity measurements obtained from cylindrical specimens (Ø100×200 mm). The SER results (Fig. 4a) demonstrate minimal variation across EPP substitution levels, with mean values of 51.6 kΩ·cm (range: -5.4/+3.3), 68.2 kΩ·cm (range: -4.9/+9.6), and 79.5 kΩ·cm (range: -5.4/+8.0) at 7, 28, and 56 days respectively. These results confirm that calcite replacement by EPP (0-100% vol.) had statistically insignificant effects ($p>0.05$) on SER, with all mixtures consistently exhibiting very low chloride ion penetration susceptibility ($37<SER\leq254$ kΩ·cm) per ASTM C1876 classification (AASHTO TP 95, 2014). BER measurements (Fig. 4b) showed comparable stability, recording mean values of 170.3 kΩ·cm (range: -10.3/+7.4), 235.5 kΩ·cm (range: -16.9/+12.8), and 282.4 kΩ·cm (range: -28.1/+34.6) at equivalent testing ages. The narrow standard deviations (±<15% of mean values) and classification as negligible penetration risk (BER>190 kΩ·cm) (Zulkarnain and Ramli, 2008) further substantiate that EPP incorporation maintains the dense microstructure characteristic of UHPC systems.

3.5 Thermal conductivity

In addition to the reduction in the unit weight of concrete, the use of lightweight aggregates in concrete also leads to a reduction in the thermal conductivity of the material. For this reason, this property was determined in this work in concretes with and without fibers to determine both the effect of the EPP dosed in different quantities, as well as the effect of the synthetic fiber.

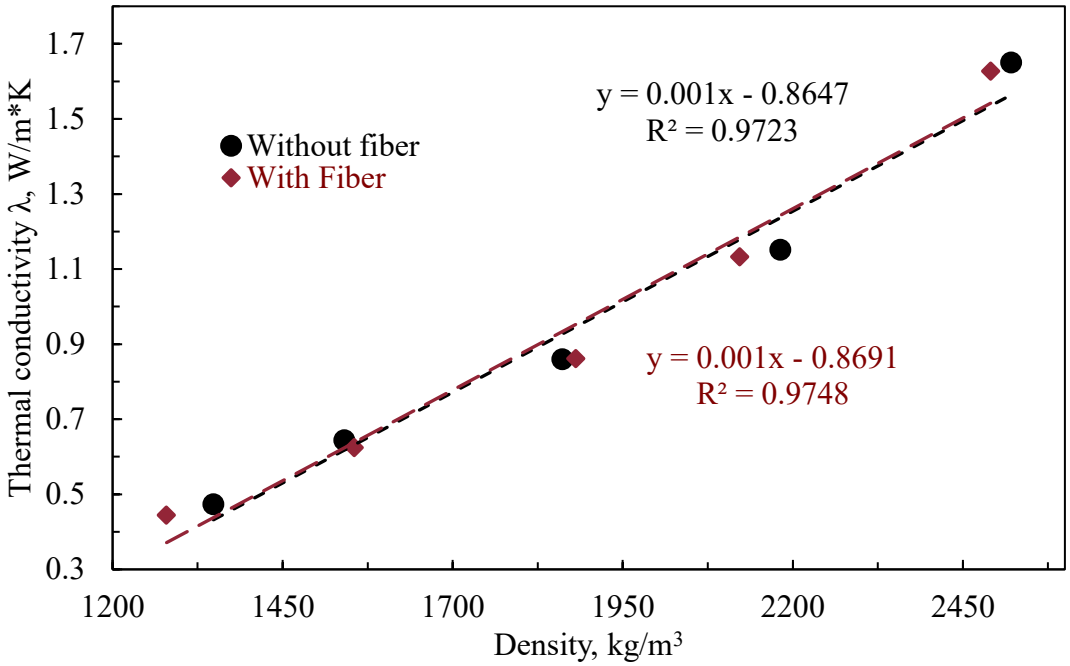

Figure 5. Influence of different percentages of EPP on thermal conductivity.

As can be seen in Figure 5, the thermal conductivity has a very good correlation with the density of the concrete and decreases as the volumetric weight of the concrete decreases, at a rate of 1 × 10-3 for each kg/m^3 of concrete. We can also observe that the results for the concretes with fiber were practically the same as those of the concretes without fiber, since they presented the same rate of decrease in thermal conductivity in relation to the decrease in volumetric weight, which indicates that, for the quantities of fiber dosed, the influence of the fiber was negligible.

4. CONCLUSIONS

From the results obtained in this research work, the following conclusions can be drawn:

1. The rapid compressive strength gain observed within the first three days (79–89% of 28-day strength) is attributed to the synergistic effect of the low water-cementitious ratio (w/cm = 0.22) and high reactivity of the cement-metakaolin system. Notably, the 100% EPP mixture achieved 22 MPa at 56 days, meeting the minimum structural requirement (17 MPa per ACI 318-19) by 7 days, validating its suitability for quality-controlled prefabricated applications.
2. EPP substitution reduced first-crack loads by 30–71% (vs. reference mix), but PVA fibers (1.5–2.0% vol.) effectively restored post-cracking capacity, particularly during strain softening. The 1.5% PVA dosage improved residual strength by up to 29%, demonstrating its critical role in maintaining structural integrity under flexural stresses.
3. SER (51.6–79.5 kΩ·cm) and BER (170.3–282.4 kΩ·cm) results confirmed that EPP incorporation (0–100%) had negligible impact on chloride resistance, with all mixtures classified as "very low" (SER) or "negligible" (BER) penetration risk per ASTM/AASHTO standards. This affirms the durability consistency of EPP-UHPC, a key quality assurance metric.
4. Thermal conductivity exhibited a linear inverse correlation with density ($\lambda = -1\times10^{-3}$ W/m·K per kg/m³, $R^2 > 0.95$), enabling predictable performance control for insulating lightweight applications. The 30% EPP mix optimized this balance (1.1 W/m·K at 1950 kg/m³).
5. This work provides a QC compliant framework for L-UHPC production, ensuring compliance with mechanical (ACI 318-19), durability (ASTM C1876), and thermal performance criteria for architectural-structural hybrid elements.

5. ACKNOWLEDGMENTS

We would like to acknowledge Filiberto Marin-Lopez from EUCOMEX for the donation of SP and STA admixtures, to Humberto Cantu from KURARAY Mexico for the donation of the PVA fibers, and to the Consejo Nacional de Humanidades, Ciencia y Tecnología (CONAHCYT), for the scholarship awarded to Jorge Xilotl so that he could carry out his master's studies with an emphasis on construction materials at UANL.

6. REFERENCES

Abu, Y., Sulaiman, D., Akeed, M., Qaidi, S., Tayeh, B. (2022). *Influence of polypropylene and steel fibers on the mechanical properties of ultra-high-performance fiber-reinforced geopolymer concrete.* Case Studies in Construction Materials, Volume 17, e01234, ISSN 2214-5095, https://doi.org/10.1016/j.cscm.2022.e01234.

Akeed, M., Qaidi, S., Ahmed, H., Faraj, R., Mohammed, A., Mahmood, W., Tayeh, B., Azevedo, A. (2022). *Ultra-high-performance fiber-reinforced concrete. Part IV: Durability properties, cost assessment, applications, and challenges.* Case Studies in Construction Materials. 17. e01271. https://doi.org/10.1016/j.cscm.2022.e01271.

Alkadhim, H. A., Amin, M. N., Ahmad, W., Khan, K., Umbreen-us-Sahar, Al-Hashem, M. N., Mohamed, A. (2022) *An overview of progressive advancement in ultra-high performance concrete with steel fibers.* Front. Mater. 9:1091867. doi: https://doi.org/10.3389/fmats.2022.1091867

Andrade, C., D'Andrea, R. (2011). *La resistividad eléctrica como parámetro de control del hormigón y de su durabilidad.* Revista de la Asociación Latinoamericana de Control de Calidad, Patología y Recuperación de la Construcción, 1(2), 93-101.

AASHTO TP 95 (2014), "*Standard Test Method for Surface Resistivity of Concrete's Ability to Resist Chloride Ion Penetration,*" American Association of State Highway and Transportation Officials, Washington, DC, 10 pp.

Azmee, N. M., Shafiq, N. (2018). *Ultra-High-Performance Concrete: From Fundamental to Applications.* Case Studies in Construction Materials. doi: https://doi.org/10.1016/j.cscm.2018.e00197

Badogiannis, E., Maria, S., Konstantinos, A., Alexandros, C. (2021). *Durability of Structural Lightweight Concrete Containing Different Types of Natural or Artificial Lightweight Aggregates.* Corrosion and Materials Degradation 2, no. 4: 554-567. https://doi.org/10.3390/cmd2040029.

Bozorgmehr, S., Nemati, M. (2023). *Applied development of sustainable-durable high-performance lightweight concrete: Toward low carbon footprint, durability, and energy saving,* Results in Materials, Volume 20, 100482, ISSN 2590-048X, https://doi.org/10.1016/j.rinma.2023.100482.

Chung, S.-Y., Sikora, P., Kim, D. J., El Madawy, M. E., Abd Elrahman, M. (2021). *Effect of different expanded aggregates on durability-related characteristics of lightweight aggregate concrete.* Materials Characterization, 173, 110907. doi: https://doi.org/10.1016/j.matchar.2021.110907.

Dixit, A., Pang, S. D., Kang, S.-H., Moon, J. (2019). *Lightweight structural cement composites with expanded polystyrene (EPP) for enhanced thermal insulation.* Cement and Concrete Composites. doi: https://doi.org/10.1016/j.cemconcomp.2019.04.023

Dong, Y. (2018). *Performance assessment and design of ultra-high-performance concrete (UHPC) structures incorporating life-cycle cost and environmental impacts.* Construction and Building Materials, 167, 414–425. doi: https://doi.org/10.1016/j.conbuildmat.2018.02.037

Du, J., Meng, W., Khayat, K. H., Bao, Y., Guo, P., Lyu, Z., Wang, H. (2021). *New development of ultra-high-performance concrete (UHPC).* Composites Part B: Engineering, 224, 109220. doi: https://doi.org/10.1016/j.compositesb.2021.109220

FM 5-578 (2004), "*Florida Method of Concrete Resistivity as an Electrical Indicator of its Permeability*", Florida, U.S.A

Gasparri, E., Brambilla, A., Lobaccaro, G., Goia, F., Andaloro, A. Sangiorgio, A. (2022). *Rethinking Building Skins - Facade Tectonics Institute*

Gong, J., Ma, Y., Fu, J., Hu, J., Ouyang, X., Zhang, Z., Wang, H. (2022). *Utilization of fibers in ultra-high performance concrete: A review. Composites Part B: Engineering.* Volume 241, 109995, ISSN 1359-8368, https://doi.org/10.1016/j.compositesb.2022.109995.

Habil, M., Fehling, E. (2005). *Ultra-High-Performance Concrete: Research, Development and Application in Europe.* ACI Special Publication. 228.

Huang, H., Teng, L., Gao, X., Khayat, K., Wang, F., Liu, Z. (2022). *Use of saturated lightweight sand to improve the mechanical and microstructural properties of UHPC with fiber alignment.* Cement and Concrete Composites, Volume 129, 104513, ISSN 0958 9465, https://doi.org/10.1016/j.cemconcomp.2022.104513.

Kishore, M., Yadav, H., Garg, A. (2015). *Architectural Use of Precast Ultra High-Performance Concrete.* International Journey of Scientific Research. ISSN 2277 – 8179

Le, A., Ekkehard, F. (2017). *Influence of steel fiber content and aspect ratio on the uniaxial tensile and compressive behavior of ultra high performance concrete.* Construction and Building Materials. 153. 790-806. https://doi.org/10.1016/j.conbuildmat.2017.07.130.

Li, Y., Zhan, G., Yang, J., Ding, Y., Ding, Q., Wang, Y. (2022). *Chloride Ion Transport Properties in Lightweight Ultra-High-Performance Concrete with Different Lightweight Aggregate Particle Sizes*. Materials 15, no. 19: 6626. https://doi.org/10.3390/ma15196626.

Lu, J., Shen, Pe., Ali, H., Poon, C. (2022). Mix design and performance of lightweight ultra-high-performance concrete. Materials & Design. https://doi.org/10.1016/j.matdes.2022.110553

Market Research Report (2023). *Trends in the Façade Systems Market - Coherent Market Insights Code: CMI6229.* Recuperado de: https://www.coherentmarketinsights.com/industry-reports/facade-systems-market

Mazzacane, P., Ricciotti, R., Lamoureux, G., Corvez, D. (2013). *Roofing of the stade Jean Bouin in UHPFRC.* In Proceedings of international Symposium on ultra-high performance fibre-reinforced concrete (pp. 59-68)

Meng, W., Khayat, K. (2017). *Effects of saturated lightweight sand content on key characteristics of ultra-high-performance concrete.* Cement and Concrete Research, 101, 46–54. doi: https://doi.org/10.1016/j.cemconres.2017.08.018

Noushini, A. Samali, B., Vessalas, K. (2013). *Flexural Toughness and Ductility Characteristics of Polyvinyl Alcohol Fibre Reinforced Concrete (PVA-FRC).* Proceedings of the 8th International Conference on Fracture Mechanics of Concrete and Concrete Structures, FraMCoS 2013. 1110-1121.

Perry V. (2018). *What really is ultra-high performance concrete – towards a global definition.* In: Proceedings of the 2nd international conference on UHPC materials and structures. Fuzhou: RILEM Publications.

Shi, C., Wu, Z., Xiao, J., Wang, D., Huang, Z., Fang, Z. (2015). *A review on ultra high performance concrete: Part I. Raw materials and mixture design.* Construction and Building Materials, 101, 741–751. doi: https://doi.org/10.1016/j.conbuildmat.2015.10.088

Siwinski, J., Szczeniak, A., Stolarski, A. (2020). *Modified Formula for Designing Ultra-High-Performance Concrete with Experimental Verification*. MDPI Journal Materials, Materials, 13, 4518. https://doi.org/10.3390/ma13204518

Soliman, N. A., Tagnit-Hamou, A. (2017). *Partial substitution of silica fume with fine glass powder in UHPC: Filling the micro gap*. Construction and Building Materials, 139, 374–383. doi: https://doi.org/10.1016/j.conbuildmat.2017.02.084

Thienel, K.-C., Haller, T., Beuntner, N. (2020). *Lightweight Concrete – From Basics to Innovations.* Materials, 13, 1120. https://doi.org/10.3390/ma13051120

Umbach, C., Wetzel, A., Middendorf, B. (2021). *Durability Properties of Ultra-High Performance Lightweight Concrete (UHPLC) with Expanded Glass.* Materials 14, no. 19: 5817. https://doi.org/10.3390/ma14195817.

Wang, X., Wu, D., Geng, Q., Hou, D., Wang, M., Li, L., Wang, P., Chen, D., Sun, Z. (2021). *Characterization of sustainable ultra-high-performance concrete (UHPC) including expanded perlite.* Construction and Building Materials, 303, 124245. doi: https://doi.org/10.1016/j.conbuildmat.2021.124245

Weina, M., Samaranayake, V., Khayat, K. (2018). F*actorial design and Optimization of Ultra-High-Performance Concrete with Lightweight Sand.* ACI materials Journal. ResearchGate. DOI: https://doi.org/10.14359/51700995

Wetzel, A., Umbach, C., Ekkehard, F., Middendorf, B. (2016). *Multifunctional prefabricated walls made of UHPC and foam concrete.*

Yang, J., Chen, B., Su, J., Xu, G., Zhang, D., Zhou, J. (2022). *Effects of fibers on the mechanical properties of UHPC: A review. Journal of Traffic and Transportation Engineering (English Edition)*, Volume 9, Issue 3, Pages 363-387, ISSN 2095-7564, https://doi.org/10.1016/j.jtte.2022.05.001.

Zulkarnain, F., Ramli, M. (2008). *Durability performance of lightweight aggregate concrete for housing construction. 2nd international conference on built environment in developing countries.* Recuperado de: https://core.ac.uk/download/pdf/83543337.pdf